Zhou Mengyang (Orcid ID: 0000-0002-2155-506X)
Granger Julie (Orcid ID: 0000-0001-9985-9242)
Chang Bonnie X. (Orcid ID: 0000-0002-5887-8655)

Influence of sample volume on nitrate N and O isotope ratio analyses with the denitrifier method

Mengyang Zhou[1], Julie Granger[1], Bonnie X. Chang[2]

[1]Department of Marine Sciences, University of Connecticut, Groton, CT, USA

[2]Cooperative Institute for Climate, Ocean, and Ecosystem Studies, University of Washington, Seattle, WA, USA

Correspondence

M. Zhou, Department of Marine Sciences, University of Connecticut, Groton, CT, USA. Email: mengyang.zhou@uconn.edu

Keywords: denitrifier method, nitrate, stable isotope

Rationale: Analyses of the isotope ratios of nitrogen ($^{15}N/^{14}N$) and oxygen ($^{18}O/^{16}O$) in nitrate (NO_3^-) with the denitrifier method require relatively high sample volumes at low concentrations (≤ 1 µM) to afford sufficient analyte for mass spectrometry, resulting in isotopic offsets compared to more concentrated samples of the same isotopic composition.

Methods: To uncover the origins of isotopic offsets, we analyzed the N and O isotope ratios of the NO_3^- reference materials spanning concentrations of 0.5 - 20 µM. We substantiated the incidence of volume-dependent isotopic offsets, then investigated whether they resulted from (a) incomplete sample recovery during N_2O sparging, (b) blanks – bacterial, atmospheric, or in reference material solutions – and (c) oxygen atom exchange with water during the bacterial conversion of NO_3^- to N_2O.

Results: Larger sample volumes resulted in modest offsets in $\delta^{15}N$, but substantial offsets in $\delta^{18}O$. N_2O recovery from sparging was less complete at higher volumes, resulting in decreases in

This is the author manuscript accepted for publication and has undergone full peer review but has not been through the copyediting, typesetting, pagination and proofreading process, which may lead to differences between this version and the Version of Record. Please cite this article as doi: 10.1002/rcm.9224

$\delta^{15}N$ and $\delta^{18}O$ due to associated isotope fractionation. Blanks increased detectably with volume, whereas oxygen atom exchange with water remained constant within batch analyses, being neither sensitive to sample volume nor salinity. The sizeable offsets in $\delta^{18}O$ with volume are only partially explained by the factors considered in our analysis.

Conclusion: Our observations argue for bracketing of NO_3^- samples with reference materials that emulate sample volumes (concentrations) to achieve improved measurement accuracy and foster inter-comparability.

1. INTRODUCTION

The isotope ratios of nitrogen ($^{15}N/^{14}N$) and oxygen ($^{18}O/^{16}O$) in nitrate (NO_3^-) are routinely measured in environmental samples using the denitrifier method developed by Sigman et al. (2001)[1] and Casciotti et al. (2002).[2] Denitrifying bacteria that lack nitrous oxide (N_2O) reductase activity quantitatively convert NO_3^- to nitrous oxide gas (N_2O), followed by cryogenic capture and analysis of $^{15}N/^{14}N$ and $^{18}O/^{16}O$ of N_2O on a gas chromatograph isotope ratio mass spectrometer. With a complete conversion of NO_3^- to N_2O, the $^{15}N/^{14}N$ of the N_2O end-product is that of the initial NO_3^- due to a mass balance of N. The $^{18}O/^{16}O$ of the N_2O end-product derives from that of the initial NO_3^-, accounting for (a) "branching" isotope fractionation whereby lighter O isotopes are preferentially lost as water and only one of six O atoms in the original NO_3^- is transferred to N_2O, and (b) O atom exchange with water during denitrification (Fig. 1). The N and O isotope ratios of NO_3^- are typically reported in delta notation (δ), versus an internationally recognized isotopic standard:

$$\delta^{14}N = \frac{(^{15}N/^{14}N)_{sample}}{(^{15}N/^{14}N)_{standard}} - 1 \quad (1)$$

$$\delta^{18}O = \frac{(^{18}O/^{16}O)_{sample}}{(^{18}O/^{16}O)_{standard}} - 1 \quad (2)$$

The δ values are reported in units of per mil (‰) versus a recognized standard. The standard for N is N_2 gas in air, and for O is Vienna Standard Mean Ocean Water (VSMOW).

The denitrifier method realizes relatively rapid and sensitive measurements of natural abundance NO_3^- isotope ratios at concentrations ≥ 1-2 µM, with a median precision of ±0.1‰ for N and ±0.3‰ for O in our laboratory. It has been widely used to measure NO_3^- isotope ratios of samples from various environments, including seawater,[3] groundwater[4,5] and soil extracts.[6] It has also been adapted to quantify the $^{15}N/^{14}N$ of organic nitrogen following its oxidation to NO_3^-, including dissolved organic nitrogen,[7] organic nitrogen from flow cytometry sorted phytoplankton populations[8] and organic nitrogen bound in calcium carbonate and siliceous fossil material.[9] Since its inception, modifications of the method have improved its throughput and precision, and lowered the requisite amount of N analyte while retaining high precision.[10,11]

Although the denitrifier method boasts a high precision, measurement accuracy is potentially subject to matrix effects, which are not universally heeded. Specifically, NO_3^- isotope ratio measurements, particularly the O isotope ratios, are sensitive to sample concentration and/or the corresponding sample volume: A fixed amount of NO_3^- is typically aliquoted to bacterial concentrates to yield a constant amount of N_2O analyte in order to mitigate source linearity and to yield constant sample to blank ratios. Most instrumental configurations require sample sizes of 10 to 20 nmoles of N to achieve adequate resolution, although some configurations enable quantitation of ≥ 3 nmoles of N.[11] Low-concentration samples may thus require relatively large sample volumes, in excess of 10 mL. In spite of the constant amount of analyte introduced into the ionization source, volume/concentration-dependent offsets in isotope ratios are often observed, particularly in O isotope ratios: Weigand et al. (2016)[11] documented concentration- (i.e., volume-) dependent differences in the $\delta^{18}O$ values of NO_3^- for reference materials spanning a range of concentrations from 15 to 200 µM (at 0.1 to 1.3 mL sample volumes). The authors argued that modest offsets on NO_3^- N and O isotope ratios derive from instrumental, solution and/or bacterial blanks, and postulated that more substantial concentration-dependent offsets arise due to O atom exchange with water. They concluded that sample analyses should be bracketed with NO_3^- reference materials of corresponding

concentrations. Conversely, McIlvin and Casciotti (2011)[10] reported sizeable shifts in $\delta^{15}N$ of NO_3^- reference materials with a relatively elevated $\delta^{15}N$ of 180‰ vs. air (USGS-32) and otherwise argued for an important influence of contaminant NO_3^- in the seawater into which reference materials were diluted. The authors advocated for bracketing samples with concentrated NO_3^- reference solutions (~200 µM) to minimize the influence of solution blanks, rather than bracketing with reference materials of comparable concentrations. In light of these apparently conflicting results and recommendations, we submit that the cause(s) of isotope offsets remain equivocal, as do the best means of accounting for these.

Here, we seek to ascertain origin(s) of volume/concentration-dependent offsets (henceforth referred to as "volume-dependent" offsets) in isotope ratios measured with the denitrifier method in order to arrive at decisive and indisputable recommendations to ensure accuracy and inter-comparability of NO_3^- isotope ratios measurements, particularly O isotope ratios. We investigate a relatively broad range of NO_3^- concentrations and incidental sample volumes and also consider a potential influence of sample salinity on the isotope ratio measurements. Our study substantiates a volume dependence of NO_3^- isotope ratio measurements that is modest for N but considerable for O isotope ratios. We demonstrate that isotopic offsets on both N and O isotope ratios derive primarily from incomplete recovery of the N_2O analyte from sparging of higher volume samples, and from the volume-dependent contributions of different blank sources. Additional volume-dependent offsets specific to O isotope ratios are not explained by purported differences in O atom exchange with water among samples of different volumes or salinity – contrary to current notions – leading us to speculate on an unidentified process apt to modulate $\delta^{18}O$ values at higher sample volumes. We conclude that bracketing of NO_3^- samples with reference materials of comparable sample volumes (concentrations) is paramount to achieving measurement accuracy, particularly for O isotope ratios, and should thus be standard practice for analyses with the denitrifier method.

2. EXPERIMENTAL

2.1 Analysis of NO_3^- N and O isotope ratios with the denitrifier method

The denitrifying bacteria strains *Pseudomonas chlororaphis* f. sp. *aureofaciens* (ATCC 13985, Manassas, VA, USA) and *Pseudomonas. chlororaphis* (ATCC 43928, Manassas, VA, USA) were used for this study. Hereafter, we refer these as *P. aureofaciens* and *P. chlororaphis*. Both strains lack a terminal nitrous oxide reductase, and thus quantitatively convert NO_3^- to N_2O. *P. aureofaciens* is used to analyze both N and O isotopic composition of NO_3^-, whereas *P. chlororaphis* only allows for the determination of the N isotopic composition of NO_3^- due to a high degree of O atom exchange with water during denitrification. Nevertheless, we and others[11] have observed that *P. chlororaphis* is less prone to culture failure.

Cultures were inoculated from cryo-preserved aliquots[11] into sterile growth media prepared as originally described[1,2] in 700 mL glass bottles containing 600 mL of medium, then sealed with gas-tight lids. Cells were cultured for 7-10 days at 20˚C on a rotary shaker table. Cultures were harvested by centrifugation and resuspended into 220 mL of fresh medium without potassium nitrate addition[10] and containing anti-foam reagent, achieving *ca.* 3-fold concentration of the bacteria. Our cell concentrations were admittedly in the lower range than is customary (10-fold in Sigman et al. (2001)[1] and Casciotti et al. (2002);[2] 3.7- and 10- fold in McIlvin and Casciotti (2011);[10] 5 to 10-fold in Weigand et al. (2016)[11]). Two (2) mL of the cell concentrates were added to respective 20-mL headspace glass vials and capped with pre-rinsed butyl rubber septa and crimp-seals.[10] The butyl rubber septa were pre-soaked overnight in deionized water to minimize the incidence of N_2O blanks, which are thought to arise because of emanation from the butyl rubber.[11] Vials were sparged with a water-scrubbed N_2 gas stream for 6 hours to remove any N_2O produced from the residual NO_3^- in the medium, potentially longer than necessary to minimize residual N_2O.[1,10,11] NO_3^- samples were then injected into each vial to achieve a final sample size of 10 nmoles of N. A series of replicate vials with only the bacterial concentrate were included in each batch analysis to assess the incidence of "bacterial blanks."

Vials were incubated inverted in order to prevent potential N_2O leakage. Following overnight incubation in the dark, *ca.* 0.1 ml of 10 mol L^{-1} NaOH was injected into each vial to kill the cultures and sequester CO_2 into carbonate species. The N_2O gas in the vials was extracted, purified and analyzed with a Delta V Advantage continuous flow gas chromatograph isotope ratio mass spectrometer (Thermo Fisher Scientific, Waltham, MA, USA) interfaced with a modified Thermo Fisher Scientific Gas Bench sample preparation device fronted by dual cold traps[2] and a GC Pal autosampler (CTC Analytics, Zwingen, Switzerland). The sparging needle length was such that it reached the liquid surface or was fully submerged. Sample were sparged with helium for 9.5 minutes at a flow rate of 25 mL min^{-1}. Our flow rate was akin to that originally recommended by Casciotti et al. (2002),[2] while lower than the reported 30 mL min^{-1} in McIlvin and Casciotti (2011)[10] and 38 mL min^{-1} in Weigand et al. (2016).[11] Samples were referenced to pure N_2O injections from a common reference gas cylinder.

Some analyses were conducted at Princeton University, where N_2O gas in the vials was extracted, purified and analyzed with a MAT253 continuous flow gas chromatograph isotope ratio mass spectrometer (Thermo Fisher Scientific, Waltham, MA, USA) interfaced with a custom-built sample preparation devices fronted by dual cold traps[11] and a GC Pal autosampler (CTC Analytics, Zwingen, Switzerland). Samples were also referenced to pure N_2O injections from a common reference gas cylinder.

2.2 Preparation of NO_3^- reference materials

NO_3^- isotopic analyses were calibrated to internationally recognized NO_3^- reference materials IAEA-NO3 (International Atomic Energy Agency, Vienna, Austria) and USGS-34 (National Institute of Standards and Technology, Gaithersburg, MD, USA), with reported $\delta^{15}N$ values of 4.7‰ and -1.8‰ (vs. air), and $\delta^{18}O$ values of 25.6‰ and -27.9‰ (vs. VSMOW).

The reference solutions were prepared from salts into primary stocks at 200 µmol L^{-1} in deionized water (DIW) from a Milli-Q™ water purification system (EMD Millipore, Burlington,

MA, USA), and stored frozen. Working solutions were diluted from primary stocks into different solution matrices to targeted concentrations (see below), in DIW or in NO_3^--deplete seawater collected from the surface Sargasso See near Bermuda (salinity of ~35 ppt).

In order to assess the influence of sample volume on the isotope composition of the N_2O analyte deriving from respective reference materials, we report the isotope ratios of the N_2O product versus those of the industrial N_2O reference gas, $\delta^{15}N_{N2O}$ (‰ vs. N_2O_{ref}), corrected for the mass-dependent abundance of $^{14}N_2{}^{17}O$.[12] The reported $\delta^{15}N$ of industrial N_2O is akin to that of N_2 in air, and its $\delta^{18}O$ is +36 – 43‰ vs VSMOW.[13]

2.3 Analysis of trace NO_3^- concentrations

In order to ensure that NO_3^- reference materials were diluted in NO_3^--deplete solutions, trace NO_3^- analyses were performed by conversion to nitric oxide (NO) in heated vanadium (III) solution followed by detection of NO on a Chemiluminescent NOx analyzer (model T200 Teledyne Advanced Pollution Instrumentation).[14] Large volume injections (≤ 5 mL) allowed for the detection of with NO_3^- concentrations ≥ 16 nmol L^{-1}. This limit of detection (LOD) was estimated from a linear calibration curve (data not shown). $LOD = 3\sigma_b/m$, where σ_b is the standard deviation of the y-intercept, and m is the slope of the regression curve.[15]

2.4 Investigation of "volume effects" on NO_3^- N and O isotopic ratios

In order to demonstrate the influence of sample volume on resulting NO_3^- isotope ratios measured with the denitrifier method, and to uncover the basis of resulting isotopic offsets, we conducted the following tests: (1) We first analyzed the isotope composition of N_2O produced from the bacterial conversion of NO_3^- reference materials diluted in DIW or seawater at increasing concentration increments (decreasing volume) in order to demonstrate the occurrence of volume-dependent isotopic offsets. (2) We then explored whether incomplete N_2O analyte recovery during sparging of high-volume samples can explain the observed isotopic offsets. (3) We further investigated whether the observed isotopic offsets derived from N_2O

blanks originating from the bacterial concentrates, from equilibration with atmospheric N_2O, or from NO_3^- contamination of the water into which the standards were diluted. (4) Finally, we considered the influence of sample volume and sample salinity on the degree of O atom exchange with water during denitrification.

2.4.1 Demonstration of "volume effects" in analyses of NO_3^- reference materials

Primary stocks of NO_3^- reference materials (IAEA-NO3 and USGS-34) were diluted in NO_3^--deplete surface Sargasso seawater or in aged DIW to concentrations of 1, 5 and 20 µmol L^{-1}, corresponding to respective injection volumes of 10, 2 and 0.5 mL, in order to aliquot 10 nmoles of N analyte. We "aged" the DIW because that dispensed directly from our water purification system results in high N_2O blanks, an occurrence noticed by others (M. Hastings, *personal communication*). The NO_3^- aliquots were injected into the sparged bacterial concentrates of either *P. chlororaphis* or *P. aureofaciens*. Following bacterial conversion, the resulting N_2O in the reaction vials was extracted, purified and analyzed on the isotope ratio mass spectrometer.

2.4.2 Effects of sample volume on N_2O recovery and isotope analyses

Crimp-sealed vials (20 mL) containing incremental volumes (0 to 14 mL) of DIW or NO_3^--deplete seawater were sparged with N_2 gas for 30 minutes, aliquoted with N_2O gas (10 nmol N) and equilibrated for ≥ 24 hours. The N_2O gas in the vials was then extracted, purified and its N and O isotopic composition analyzed on the isotope ratio mass spectrometer.

In a parallel set of experiments conducted at Princeton University, crimp-sealed vials (20 mL) containing incremental volumes (0 to 9.3 mL) of DIW were sparged with helium gas for 30 minutes, aliquoted with N_2O gas (5 nmol N) and equilibrated on a shaker for 2 hours. The N_2O gas in the vials was then extracted with an autosampler needle that only penetrated samples ≥ 8.3 mL. N_2O thus extracted was purified and its N and O isotopic composition analyzed on an isotope ratio mass spectrometer.

2.4.3 Effects of sample volume on the size of blanks

Following sparging with N_2 gas, bacterial concentrates (2 mL) in 20 mL vials were injected with incremental volumes of DIW or NO_3^--deplete surface Sargasso seawater. Solutions included air-equilibrated DIW (for ≥ 1 day) and helium-sparged DIW (for 30 minutes), as well as air-equilibrated vs. helium-sparged seawater. N_2O yields were estimated from peak areas recovered by mass spectrometric analysis, calibrated with standard additions. The isotope composition of the blanks was not assessed, however, given the influence of source linearity on diminutive sample sizes.

2.4.4 Effects of sample volume and salinity on O atom exchange with water

To assess the influence of sample volume and seawater-driven salinity on O atom exchange with water during bacterial conversion of NO_3^- to N_2O, NO_3^- reference materials (IAEA-NO3 and USGS-34) were diluted with mixtures of DIW and NO_3^--deplete Sargasso ranging in salinity from 0 to 35 ppt to achieve NO_3^- concentrations of 1, 3, 5 and 20 µmol L^{-1} – corresponding to respective injection volumes of 10, 3.3, 2 and 0.5 mL – in order to attain 10 nmoles of N analyte. Reference materials at corresponding salinity and NO_3^- concentrations were supplemented with ^{18}O-labled water, resulting in $\delta^{18}O_{H2O}$ values ranging from -6.8 to 335‰ vs. VSMOW. The $\delta^{18}O_{H2O}$ values were calculated based on dilution of 97 atom % ^{18}O-labeled water.

3. RESULTS AND DISCUSSION

3.1 Volume-dependent offsets in NO_3^- N and O isotope ratios of reference materials

In trials with *P. aureofaciens* and *P. chlororaphis* aliquoted with 10 nmoles of respective NO_3^- reference materials, the amount of N_2O detected by the mass spectrometer decreased with sample concentration, thus with increasing sample volumes (Fig. 2a, b). N_2O peak areas were 5 - 23% lower for 10 mL sample injections than for 0.5 mL injections. The differences in N_2O peak areas of the 0.5 vs. 10 mL injections were significantly greater for DIW than for seawater samples with *P. aureofaciens* (paired two sample t-test, $t(5)=26$, $p<0.001$), but

showed no significant difference between DIW and seawater with *P. chlororaphis* (two sample t-test, t(4)=2.8, p>0.05).

The $\delta^{15}N$ values of N_2O produced from respective NO_3^- reference materials differed slightly but detectably as a function of volume, albeit, revealing different trends for analyses with *P. aureofaciens* vs. *P. chlororaphis*. For *P. aureofaciens* analyses, $\delta^{15}N$ values were similar between the 0.5 and 2 mL injections (20 and 5 µM NO_3^-) for both reference materials, but decreased slightly in the 10 mL samples (1 µM NO_3^-) by 0.5 ± 0.1‰ for IAEA-NO3 and by 0.3 ± 0.2‰ for USGS-34 (Fig. 2c). The $\delta^{15}N$ decrease from 2 to 10 mL was significantly greater for DIW than seawater samples (paired two sample t-test, t(5)=2.6, $p < 0.05$). For *P. chlororaphis* analyses, no coherent trend emerged among trials (Fig. 2d). From 0.5 to 10 mL, IAEA-NO3 values increased by 0.2 ± 0.1‰ in one trial but decreased by 0.4 ± 0.1‰ in another. The corresponding USGS-34 samples showed negligible offsets with volume.

The $\delta^{18}O$ values of N_2O from the NO_3^- reference solutions differed more dramatically with sample volume than corresponding $\delta^{15}N$ values in analyses with *P. aureofaciens* (Fig. 2e). As sample volume increased from 0.5 to 2 mL (20 to 5 µM), the $\delta^{18}O$ values for IAEA-NO3 samples changed by -0.5 to 0.7‰ among trials, while values for USGS-34 samples increased consistently by 1.2 ± 0.6‰, thus more evidently than in corresponding IAEA-NO3 samples. From 2 to 10 mL injections (5 to 1 µM), the $\delta^{18}O$ values of IAEA-NO3 samples decreased by 1.6 ± 0.7‰, while those of USGS-34 samples increased slightly by 0.3 ± 0.7‰. The volume-specific differences in $\delta^{18}O$ values were not significantly different between DIW and seawater samples (paired two sample t-test, t(5)=2.6, p>0.1).

In all trials, the percent deviation of the difference between measured $\delta^{18}O$ values of IAEA-NO3 and USGS-34 from the true difference increased with sample volume (Fig. 3a). Henceforth, we refer to this dynamic as the "$\delta^{18}O$ scale contraction." The $\delta^{18}O$ scale contraction was 3.0 ± 0.6% for the 0.5 mL injections, increasing to 5.0 ± 0.8% for the 2 mL injections, and 8.5 ± 0.8%

for the 10 mL injections. No significant difference in $\delta^{18}O$ scale contraction was detected between DIW and seawater samples (paired two sample t-test at each volume, $p > 0.4$ for all volumes). Similarly, we define $\delta^{15}N$ scale contraction as the percent deviation of the difference between measured $\delta^{15}N$ values of IAEA-NO3 and USGS-34 from the true difference (Fig. 3b). The mean $\delta^{15}N$ scale contraction among trials was 0.5 ± 0.4% for the 0.5 mL aliquots, increasing to 1.6 ± 1.4% for the 2 mL aliquots, although a volume-dependent increase was not evident in all trials. The average $\delta^{15}N$ scale contraction increased further to 3.9 ± 0.1% for the 10 mL injections. There was no significant difference in $\delta^{15}N$ scale contraction between DIW and seawater samples (paired two sample t-test, *p > 0.01* for each volume).

These observations clearly demonstrate a sensitivity of the measured N_2O isotope ratios to sample size as a function of NO_3^- concentration and/or volume of the sample aliquot. They reveal a tendency for incomplete N_2O recovery in higher volume samples, an important volume-dependent response of $\delta^{18}O$ values to sample size, and a comparatively muted response of $\delta^{15}N$ values. We note here that our observations replicate those of Weigand et al. (2016)[11] who also observed an increase of $\delta^{18}O$ values between 0.1 to 2.5 mL aliquots of IAEA-NO3 and USGS-34 reference materials; Their study, however, did not extend to higher sample volumes (i.e., lower concentrations). And they similarly reported little to no difference in $\delta^{15}N$ values over this narrower volume range.

The influence of sample volume on the isotope ratios is notably pertinent to environmental samples in the natural abundance range. Duplicate analyses of a 20 µmol L^{-1} NO_3^- sample collected at 2000 m in the Sargasso Sea (0.5 mL injection volume) corrected against respective NO_3^- reference solutions at different concentrations (i.e., injection volumes) in a unique trial returned $\delta^{15}N$ values of 4.9 ± 0.1, 4.8 ± 0.1 and 5.3 ± 0.1 ‰ *vs.* air for the 0.5, 2 and 10 mL references solutions, respectively, and corresponding $\delta^{18}O$ values of 2.2 ± 0.1, 1.5 ± 0.1 and 2.7 ± 0.1 ‰ *vs.* VSMOW.

3.2 Volume effects on N_2O recovery and isotopologue ratios

We first investigate the extent to which incomplete N_2O recovery can explain associated isotopic trends. Barring incomplete bacterial conversion to N_2O, lower N_2O yields at high volumes may then arise from incomplete sample recovery during sample sparging with our current extraction configuration, wherein a proportional fraction of the N_2O analyte remains dissolved in the sample following N_2O extraction. The observed offsets could then result from isotope fractionation between the dissolved and gas phases.

In helium-sparged vials directly aliquoted with 5 nmoles of N_2O (10 nmoles of N), the N_2O recovered generally decreased with increasing volume of DIW or seawater (Fig. 4a). N_2O peak areas decreased by approximately 0.3 to 0.9 % per mL of sample volume among trials, ostensibly from incomplete sample recovery from higher volume solutions, wherein a larger fraction of N_2O remained in solution at higher volumes. Indeed, N_2O was recovered in subsequent analyses of previously sparged samples, minimally so in low volume samples to ~0.2 nmoles of N_2O in 13 mL samples (data not shown).

The $\delta^{15}N$ and $\delta^{18}O$ signals also decreased progressively with increasing DIW or seawater volume, albeit to differing extents among trials (Fig. 4b, c). Slopes of linear regressions of the $\delta^{15}N$ values vs. aliquot volume were -0.01 to -0.03‰ per mL for Trials 1 to 5 (Table 1), amounting to a decrease of 0.01 - 0.03‰ (vs. N_2O tank) per mL of sample, whereas no trend was apparent in Trial 6. The amplitude of decreases for $\delta^{18}O$ covered a broader range than for $\delta^{15}N$, with slopes of -0.01 to as low as -0.17‰ per mL among trials (Table 1).

The decreases of $\delta^{15}N$ and $\delta^{18}O$ signals in trials showing incomplete N_2O recovery are consistent with kinetic isotope fractionation during N_2O evasion from water to the gas stream. Reported kinetic fractionation factors for ^{15}N and ^{18}O substituted N_2O ($^{15}\alpha_{evasion}$, $^{18}\alpha_{evasion}$) are 0.9993 and 0.9981 (0.7 and 1.9‰) respectively, at 25°C,[16] with lighter isotopologues evading into the gas phase more rapidly. Incomplete recovery of N_2O then results in fractionation

between the dissolved and gas phases, with progressively lower isotopic ratios of the N_2O recovered from sparging as the fraction of N_2O recovered from the dissolved phase decreases. A larger isotope fractionation factor for O isotopologues is expected *a priori* based on the greater mass difference of O compared to N isotopologues of N_2O, and is further posited to result from the short-range interaction of O atoms with the hydration sphere.[16,17] From the data shown in Figure 4, we estimated sparging isotope effects, $^{15}\alpha_{sparging}$ and $^{18}\alpha_{sparging}$ for trials in which slopes differed significantly from zero (p-value ≤ 0.01; Table 1). The estimated ranges of $^{15}\alpha_{sparging}$ and $^{18}\alpha_{sparging}$ are 0.9987 - 0.9996 (1.3 - 0.4‰) and 0.9934 – 0.9987 (6.6 - 1.3‰), respectively. Our estimates of $^{15}\alpha_{sparging}$ are close to reported values ($^{15}\alpha_{evasion}$ = 0.9993), whereas our estimates for $^{18}\alpha_{sparging}$ include values that diverge appreciably from reported estimates for N_2O evasion ($^{18}\alpha_{evasion}$ = 0.9981) – an observation that remains puzzling. Admittedly the observed sparging isotope effect here was a superposition of both kinetic and equilibrium isotope effect, yet we are uncertain as to how this can result in greater values for $^{18}\alpha_{sparging}$ than $^{18}\alpha_{evasion}$.

Differences in volume between samples and standards can thus result in isotopic offsets due to incomplete sparging of N_2O in large volume samples, resulting in progressively lower N and O isotope ratios with increasing sample volumes. The lower N_2O recovery in DIW compared to seawater samples (Fig. 2) may result from a higher solubility of N_2O in freshwater, which may explain the greater $\delta^{15}N$ decrease from 2 to 10 mL in DIW compared to seawater samples. Our sample sparging time at a flow rate of 25 mL per minute[2,10] is evidently not optimized for larger volume samples, resulting in incomplete recovery in most analyses of larger volume samples. Increasing the flow rate to reported values of 30 mL min^{-1} [10] or 38 mL min^{-1} [11] may thus be advisable. While extending the sparging time is also feasible, doing so incurs trade-offs in sample throughput. Regardless, we suspect that most instrumental configurations of the denitrifier method may have similar limitations. Indeed, Sigman and Weigand (*personal*

communication) similarly observe incomplete recovery of high volume samples and associated isotopic fractionation (Fig. 4).

We note here that our autosampler configuration (and that of Weigand et al. (2016)[11]) ensures that the sparging needle reaches the liquid phase in our samples;[10] N_2O recovery is otherwise even less effective, as demonstrated by experiments conducted at Princeton University where the sparging needle was modified such that it only penetrated samples ≥ 8.3 mL (Fig. 5). The fraction of N_2O recovered decreased dramatically with increasing volume for samples < 8.3 mL, by 2.6 ± 0.3 % per mL of sample volume compared to control vials without liquid – rather than 1.1 ± 0.8 % per mL of sample volume in our experiments with a longer needle. $\delta^{15}N$ and $\delta^{18}O$ values also decreased, by 0.02 ± 0.01‰ and 0.04 ± 0.02‰ per mL of sample volume, respectively. Estimated $^{15}\alpha_{sparging}$ and $^{18}\alpha_{sparging}$ from these results were 0.9994 ± 0.0001 and 0.9990 ± 0.0002, respectively, in the range reported for N_2O evasion.[16] In samples with volumes ≥ 8.3 mL, wherein the sparging needle reached the liquid, the recovered N_2O increased relative to the 7.3 mL samples, as did the corresponding $\delta^{15}N$ and $\delta^{18}O$.

Incomplete sparging of larger volume samples, while evident from incomplete analyte recovery from denitrifier vials, does not, by itself, explain the isotopic trends in Figure 2. Specifically, $\delta^{15}N$ values decreased to different extents for IAEA-NO3 and USGS-34 with increasing volume (for samples processed with *P. aureofaciens*); Isotopic fractionation should expectedly impart isotopic offsets of similar amplitude for both IAEA-NO3 and USGS-34, thus suggesting that additional factors contributed to the respective $\delta^{15}N$ offsets. The incoherent trends for *P. chlororaphis* samples, in turn, likely result from differences in the extent of O atom exchange with water among samples; Uncertainties in the estimate of O isotope exchange are propagated in the associated correction for the contribution of $^{14}N^{14}N^{17}O$ to mass 45 peak. We thus focus our analysis on *P. aureofaciens*, which showed more systematic trends.

Isotopic fractionation due to incomplete N_2O recovery also fails to fully explain volume-dependent $\delta^{18}O$ offsets in analyses with *P. aureofaciens*. At higher sample volumes, $\delta^{18}O$ values decreased to different extents for IAEA-NO3 and USGS-34, contrary to a priori expectations of equivalent decreases for isotopic fractionation imparted by incomplete sample sparging. It follows that incomplete N_2O recovery also fails to account for the increase in $\delta^{18}O$ scale contraction with sample volume (Fig. 3), which cannot be explained by incomplete sample recovery. Additional dynamics evidently influence N and O isotopologue ratios as a function of sample concentration/volume.

3.3. Volume effects on blanks and O atom exchange with water

Isotopic offsets for N and O isotope ratios of NO_3^- could arise from the incidence of blanks. For one, some N_2O remains in the bacterial concentrate following the 6 hours of sparging with N_2 gas. This bacterial blank, however, is not expected to increase with sample volume, thus imparting a conserved blank-to-sample ratio among analyses (i.e., no volume dependence of blank size). Blanks that are specifically volume-dependent could otherwise arise from atmospheric N_2O in equilibrium with the sample, or from contaminant NO_3^- in the solutions into which the reference materials are diluted.

Volume-dependent isotopic offsets, specifically those on $\delta^{18}O$, could also result from differential O atom exchange with water during denitrification. The nitrite (NO_2^-) intermediate during the bacterial conversion of NO_3^- to N_2O can undergo O isotope exchange with water, rapidly so at lower pH[18,19] and/or when biologically facilitated.[2,20,21] This dynamic explains the tendency for bacterial conversion with *P. chlororaphis* to retain only a small fraction (≤ 39%) of the original NO_3^- $\delta^{18}O$ during bacterial conversion to N_2O, whereas *P. aureofaciens* facilitates much lower isotopic exchange with water, typically ranging between 2.4 - 8.7% among batch analyses.[2]

In order to fully explore the influence of blanks and O atom exchange on O isotope ratio analyses, we consider the O isotope mass balance for the bacterial conversion of sample NO_3^- to N_2O. Given complete conversion of NO_3^- to N_2O, the resulting $\delta^{18}O$ of N_2O is influenced by isotopic fractionation, O atom exchange with water and blanks:[2]

$$m = s + b \quad (3)$$

$$\delta^{18}O_{m-N2O}m = (\delta^{18}O_{NO3} + {}^{18}\epsilon)s(1-x) + (\delta^{18}O_{H_2O} + {}^{18}\epsilon_{eq.NO2})sx + \delta^{18}O_{b-N2O}b \quad (4)$$

The term m is the total amount of N measured as N_2O, s is the amount of sample N added as NO_3^- and b is the amount of blank N_2O remaining from the bacterial preparation or introduced with the sample from equilibration with atmospheric N_2O. We note that this blank term does not account for the incidence of contaminant NO_3^- in reference material solutions, which we address further below. $\delta^{18}O_{m-N2O}$ and $\delta^{18}O_{NO3}$ designate the measured (as N_2O) and true (as NO_3^-) $\delta^{18}O$ values (‰ vs. VSMOW) of a given sample. $\delta^{18}O_{H_2O}$ and $\delta^{18}O_{b-N2O}$ are the respective $\delta^{18}O$ values of water and the N_2O blank. ${}^{18}\epsilon$ is the O isotope fractionation during the conversion of NO_3^- to N_2O. ${}^{18}\epsilon_{eq.NO2}$ is the equilibrium isotope effect associated with O atom exchange between NO_2^- and water. Given an *a priori* assumption that the values of ${}^{18}\epsilon$, b and $\delta^{18}O_{b-N2O}$ are constant within the same experimental batch analysis (a notion that we challenge with respect to *b*), Eq. 4 can be rearranged to calibrate isotope analyses to recognized reference materials from measurements of two NO_3^- reference materials with known $\delta^{18}O$ values:

$$\delta^{18}O_{NO3-ref,1} - \delta^{18}O_{NO3-ref,2} = (\delta^{18}O_{m,1} - \delta^{18}O_{m,2})(s+b)/(s(1-x)) \quad (5)$$

$\delta^{18}O_{m,1}$ and $\delta^{18}O_{m,2}$ are measured $\delta^{18}O$ values (‰ vs. VSMOW) of the respective NO_3^- reference materials, and $\delta^{18}O_{NO3-ref,1}$ and $\delta^{18}O_{NO3-ref,2}$ are their assigned $\delta^{18}O$ values (‰ vs. VSMOW). Let *k* be the ratio of the assigned $\delta^{18}O$ and measured $\delta^{18}O$ difference between the two reference materials,

$$k = (\delta^{18}O_{NO3-ref,1} - \delta^{18}O_{NO3-ref,2})/(\delta^{18}O_{m,1} - \delta^{18}O_{m,2}) \quad (6)$$

The value of *x*, the fraction of NO_3^- that undergoes O atom exchange with water, can be expressed as follows:

$$x = (sk - s - b)/(sk) \quad (7)$$

The $\delta^{18}O$ contraction, *c*, then represents the deviation (in percent) of the difference between measured $\delta^{18}O$ values of IAEA-NO3 and USGS-34 from the true difference:

$$c = 1 - 1/k = 1 - s(1 - x)/(s + b) \quad (8)$$

The $\delta^{18}O$ scale contraction, *c*, thus increases with increasing N_2O blank size, *b* or with increasing O atom exchange with water, *x*. Within a batch analysis, a sensitivity of scale contraction to sample volume may thus be conferred from volume-dependent differences in *b* and/or in *x*. If b is not constant within the same batch analysis, k differs among samples, such that batch analyses cannot be calibrated assuming a uniform value of k.

In addition to these sensitivities, scale contraction can also arise from a NO_3^- blank in the reference solutions, in which case Eq. 4 can be modified as follows:

$$\delta^{18}O_{m-N2O}(m + b_{NO3}) = [(\delta^{18}O_{NO3} + {}^{18}\epsilon)s + (\delta^{18}O_{b-NO3} + {}^{18}\epsilon)b_{NO3}](1 - x) + (\delta^{18}O_{H_2O} + {}^{18}\epsilon_{eq.NO2})(s + b_{NO3})x + \delta^{18}O_{b-N2O}b \quad (9)$$

The terms b_{NO3} and $\delta^{18}O_{b-NO3}$ represent the amount of N and $\delta^{18}O$ value (‰ vs. VSMOW) of a putative NO_3^- blank in the reference solutions, respectively. For a given volume of reference material, the values of b_{NO3} and $\delta^{18}O_{b-NO3}$ will be constant among analyses, and Eq. 8 can be modified to the following:

$$c = 1 - s(1 - x)/(s + b + b_{NO3}) \quad (10)$$

Thus, the presence of a NO_3^- contaminant in the reference solutions also decreases the difference between $\delta^{18}O_{m,1}$ and $\delta^{18}O_{m,2}$ and increases the $\delta^{18}O$ scale contraction, albeit only for the reference solutions but not the samples. Given different volume aliquots of reference

solutions, the amplitude of b_{NO3} will increase with volume – and could thus account for a volume-dependence of scale contraction. To properly address how to best calibrate sample analyses thus requires that the origin(s) and respective amplitudes of blanks be identified, and the sensitivity of O atom exchange with water to sample matrix explicitly investigated.

3.3.1 Amplitude of blanks

In repeat trials, the amount of N_2O detected in the *P. aureofaciens* and *P. chlororaphis* blanks generally increased with the volume of air-equilibrated water aliquoted to the bacterial suspensions (Fig. 6). The N_2O ranged from 0.02 to 0.08 nmoles of N in bacterial suspensions without sample aliquots to values between 0.12 and 0.46 nmoles of N in 10 mL water aliquots. Blank sizes covered comparable ranges between *P. aureofaciens* and *P. chlororaphis* trials. Blanks were roughly similar between DIW and seawater in a parallel trial with *P. aureofaciens*, but differed in a trial with *P. chlororaphis,* with higher blanks evident in the single DIW trial.

When seawater and DIW solutions were sparged with helium gas prior to injection into the bacterial suspensions, N_2O blank sizes decreased to nearly uniform values among sample volumes in the majority of trials, suggesting that the concentration dependence of blank size arises from N_2O in equilibrium with the atmosphere. Coherently, the amount of N_2O recovered from air-equilibrated DIW and seawater samples increased with volume among trials, with a median slope of 0.017 nmol N mL^{-1} (range of 0.008 to 0.040 nmol N mL^{-1}; Table 2), which is of the magnitude expected from equilibration with atmospheric N_2O of ~0.013 nmol N mL^{-1}.[22] While the slopes of the fitted regressions evince the incidence of volume-dependent blanks from atmospheric N_2O, the intercepts tended to differ among trials, ranging from 0.02 to 0.16 nmoles of N (Table 2). The magnitude of the intercepts can be ascribed to the amount of N_2O transferred with the bacterial suspensions, thus accounting for a roughly constant amount of N_2O independent of sample volume within individual batch analyses.

In a few trials, the volume-dependent increase in N_2O followed a steeper trajectory than expected from increments of atmospheric N_2O (Table 2). The steeper increase with volume suggests additional volume-dependent blanks in those trials specifically, potentially from contaminant NO_3^- in the reference material solutions. The NO_3^- in the stock seawater solutions was ≤ 16 nM at the onset. The sum of this detection limit and atmospheric N_2O amounts to an expected slope of 0.029 nmol N mL^{-1}, which is higher than the volume-dependent increases we observed in most trials, suggesting a lower concentration of contaminant NO_3^- than our limit of detection (16 nM) in most trials. The single trial with steepest slope of 0.040 nmol N mL^{-1} (Trial 190419) may thus result from a NO_3^- contaminant introduced during manipulations.

The sum of these observations suggests that the N_2O blanks detected with the denitrifier method arise primarily from the N_2O transferred with the bacterial suspension and from atmospheric N_2O in equilibrium with the samples. Secondarily, volume-dependent blanks may arise from trace NO_3^- contaminants in the water used in the preparation isotopic reference materials, or from NO_3^- contaminants subsequently introduced during handling. The increase in blank size with volume results in progressively greater blank to sample ratio, thus greater N and O isotopic offsets relative to lower volume samples. In turn, the greater $\delta^{18}O$ scale contraction observed between IAEA-NO3 and USGS-34 $\delta^{18}O$ measurements at higher volumes (Fig. 2 & 3) is explained, at least in part, by a larger N_2O blank at higher sample volumes (Eq. 8). It could also be exacerbated by greater O isotope exchange with water at higher sample volumes. We examine this hypothesis in the following section.

An increase in blank size with "NO_3^--free" seawater and DIW sample volume was observed in the original denitrifier method paper,[1] with a mean slope of ~0.03 nmol N mL^{-1} and a larger median intercept of ~0.45 nmoles N for 2 mL bacterial aliquots. The volume dependence of blanks was tentatively attributed to the desorption of N_2O from the bacteria biomass, occurring to greater extent at greater dilution; Dissolved atmospheric N_2O was ruled out as a source of

the volume-dependent blanks because sparging the NO_3^--free seawater with N_2 gas did not result in a detectable reduction in blank size. Here, while we otherwise saw reductions of the blanks for samples sparged with helium, we obtained similar results to those of Sigman et al. (2001)[1] when sparging with N_2 gas (Fig. S1). We surmise from this perplexing result that commercial N_2 gas may have trace amount of NO_x contaminants. More recently, Weigand et al. (2016)[11] also documented a volume-dependent increase in blank size of 0.015 – 0.020 nmol N mL^{-1} for low-NO_3^- seawater sample from 0 to 4 mL (Fig. 6a, b) – akin to the results observed here – which they attributed generically to contaminant NO_3^- in the reference solutions and atmospheric N_2O. The $NO_3^- + NO_2^- + N_2O$ concentration in the low-NO_3^- seawater they used was estimated to be 18 nM. As in this study, they observed a volume-independent blank of ~0.06 nmol originating from the bacterial concentrate (1.5 mL) – of the order observed here of 0.02 to 0.16 nmoles for 2 mL of bacterial concentrate. More recent analyses with *P. aureofaciens* from Weigand and Sigman (*personal communication*) reveal an intercept of 0.08 nmoles N for 1.5 mL bacterial concentrate and a slope of 0.025 nmol N mL^{-1}, also in the range of our estimates here (Fig. 6a). Our observation on the amplitude of blanks thus roughly concurs with those observed by other groups.

McIlvin and Casciotti (2011)[10] otherwise attributed blanks exclusively to the N_2O transferred with the bacterial concentrate (0.04 – 0.08 nmoles of N) and to contaminant NO_3^- of ~20 nM in the reference material solutions, based on which they recommended bracketing sample analyses with highly concentrated NO_3^- reference solutions (~200 µM) to minimize the influence of NO_3^- contaminants therein – thus matching the amount of N in coincident samples but not sample volumes. Their conclusions, however, did not address the incidence of dissolved atmospheric N_2O, which we conclude to be significant, nor the influence of sample volume on $\delta^{18}O$ scale contraction, which we investigate below.

3.3.2 Influence of sample volume and salinity on O atom exchange with water

In repeat trials with sample volumes ranging from 0.5 to 10 mL for a range of seawater salinity from 0 to 28 ppt, the fraction of O atoms in the N_2O product originated from water, *x* (Eq. 8), was estimated from the slope of the observed $\delta^{18}O_{N2O}$ vs. the corresponding $\delta^{18}O_{H2O}$. Values of *x* ranged from 0.4% to 2.9% among all trials, differing detectably among trials, but showed no coherent trend within trials with respect to sample volume and sample salinity (Fig. 7a, b). Thus, exchange appeared independent of sample volume and salinity, suggesting *a priori* that the volume-dependent $\delta^{18}O$ scale contraction observed here (Fig. 3) resulted exclusively from the incidence of blanks and not from volume-sensitive (or salinity-sensitive) differences in O atom exchange with water.

The O atom exchange values observed here are consistent with the values originally documented by Casciotti et al. (2002),[2] which ranged between 2.4%-8.7% (median ~3%) for 0.75 to 1 mL aliquots of NO_3^- reference materials. They also observed that the degree of exchange varied among batch analyses but remained constant within a given batch, and was thus independent of sample volume. However, Weigand et al. (2016)[11] later argued that the size of blanks was insufficient to explain the observed scale contraction of $\delta^{18}O$, as blanks accounted for only 0.35% of the 20 nmol N in the samples, explaining ~0.3% of their observed $\delta^{18}O$ contraction; The $\delta^{18}O$ scale contraction they observed increased from ~3% to ~4% with injection volumes of 0.1 to 1.3 mL. The authors thus surmised that the increase in $\delta^{18}O$ contraction with sample volume must otherwise arise from O atom exchange with water (Eq. 8).

We are faced here with a similar dilemma to that of Weigand et al. (2016),[11] unable to account for the observed volume-dependent increase in scale contraction given the modest size of our estimated blanks, and given our observation that the fraction of O atom exchange is independent of sample volume. For example, given 10 nmol NO_3^- aliquots, an O atom exchange fraction of 3%, a mean bacterial blank of 0.06 nmol N, an atmospheric N_2O concentration of

0.013 nmol N mL^{-1}, and a contaminant blank of 0.016 nmol N mL^{-1} in the reference solution, the $\delta^{18}O$ scale contraction would be 3.7% for the 0.5 mL samples, increasing to a maximum of 6.3% for the 10 mL samples (Model 1 in Fig. 8a). This contraction potentially explains that observed for the 0.5 mL aliquots, but is lower than observed for the 10 mL aliquots, which was typically on the order of 8%. Increasing the bacterial blank to our maximum observed value of 0.16 nmol N and prescribing the highest observed slope of blank size *vs*. volume of 0.040 nmol N mL^{-1} (presuming a contaminant NO_3^- concentration of 27 nM in the water used to prepare the reference materials, plus atmospheric N_2O) yields a scale contraction of 4.7% at 0.5 mL, somewhat higher than observed, increasing to 8.1% at 10 mL, roughly matching observations (Model 2 in Fig. 8a). Yet these parameter prescriptions derive from the highest observed values, rather than from their respective means. Moreover, the apparent "kink" in the relationship between volume and $\delta^{18}O$ scale contraction is not reproduced by any permutation.

In contrast to the $\delta^{18}O$ scale contraction, the observed $\delta^{15}N$ scale contraction is adequately reproduced by our observational constraints. A prescription of a mean bacterial blank of 0.06 nmol N, an atmospheric blank of 0.013 nmol N mL^{-1}, and a NO_3^- contaminant blank of 0.016 nmol N mL^{-1} convincingly reproduces the observed increase in $\delta^{15}N$ contraction with volume (Fig. 8a).

Compared to the $\delta^{15}N$ scale contraction, that expected for $\delta^{18}O$ should be on the order of 3.0% higher at 0.5 mL to 2.9% higher at 10 mL (Fig. 8b), close to the fraction of O atom exchange originally prescribed. This slight expected decrease with volume in the difference between $\delta^{18}O$ and $\delta^{15}N$ contraction, c_{18-15}, is explained by Eq. 10, where the $\delta^{18}O$ contraction features the exchange term ($c_{18} = 1 - s(1-x)/(s+b+b_{NO3})$), while the $\delta^{15}N$ contraction does not ($c_{15} = 1 - s/(s+b+b_{NO3})$). The value of $c_{18-15} = xs/(s+b+b_{NO3})$, thus decreases with volume due to the increase b_{NO3} and dissolved atmospheric N_2O. Contrary to expectations, however, the amplitude of c_{18-15} increased with volume, from 2.5 ± 0.3% at 0.5

mL to 4.6 ± 0.8% at 10 mL. We thus conclude that while the scale contraction for $\delta^{15}N$ analyses is adequately explained by blanks, the volume-dependent increase in scale contraction for $\delta^{18}O$ is not wholly explained by the combined influence of blanks and O atom exchange with water. We tentatively postulate that this perplexing dynamic could be due to a volume-dependent oxidation of the NO intermediate with trace molecular O_2 during denitrification,[23] or may arise from the formation of an interfering ion in the ionization source in response to increased water vapor introduced with higher volume samples.

3.4 Simulations of volume-dependent values of $\delta^{15}N$ and $\delta^{18}O$

Given the potential influences on NO_3^- N and O isotope ratios uncovered above, which include bacterial blanks, dissolved atmospheric N_2O, contaminant NO_3^- in reference materials, O atom exchange with water, and incomplete N_2O recovery and associated isotope fractionation, we attempt to account for the volume-dependent changes in $\delta^{15}N$ and $\delta^{18}O$ that we observed for IAEA-NO3 and USGS-34 reference materials (Fig. 2).

First, we reference the observed $\delta^{15}N$ and $\delta^{18}O$ values of N_2O for IAEA-NO3 and USGS-34 samples to that expected for IAEA-NO3 vs. the N_2O reference tank: We approximate the expected $\delta^{15}N$ value for IAEA-NO3 vs. N_2O_{ref} to be that observed for the highest N_2O yield (at lower aliquot volumes – which is admittedly already subject to blanks). Referenced to itself, IAEA-NO3 has a $\delta^{15}N$ of 0‰ vs. IAEA-NO3, and that expected for USGS-34 is -6.5‰ vs. IAEA-NO3. We similarly approximate the expected $\delta^{18}O$ value for IAEA-NO3 vs. N_2O_{ref} to be that observed for the highest N_2O yield. Referenced to itself, the expected $\delta^{18}O$ of IAEA-NO3 is 0‰ (vs. IAEA-NO3), and that for USGS-34 is -52.2‰ (vs. IAEA-NO3).

We first simulate the influence blanks on $\delta^{15}N$ values for IAEA-NO3 and USGS-34, accounting for (a) a bacterial blank of 0.06 nmol N, (b) atmospheric N_2O of 0.013 nmol N mL^{-1}, and (c) and NO_3^- contaminant in the solutions of 0.016 N nmol mL^{-1}. We prescribe an arbitrary $\delta^{15}N$ of 30‰ (vs. IAEA-NO3) to the bacterial blank, a value that imposes isotope fractionation of

industrial NO_3^- (initial $\delta^{15}N$ of 0‰ vs. air) due to bacterial consumption,[24] and which ultimately provides the best fit to the observations. The $\delta^{15}N$ of atmospheric N_2O is 2.1‰ (vs. IAEA-NO3)[25] and we prescribe a generic $\delta^{15}N$ of 5‰ (vs. IAEA-NO3) to the NO_3^- contaminant blank, a value in the natural abundance range. The blanks together result in a small change in the $\delta^{15}N$ of both reference materials relative to expected values, increasing IAEA-NO3 by 0.18‰ at 0.5 mL to 0.28‰ at 10 mL, compared to 0.23‰ at 0.5 mL to 0.50‰ at 10 mL for USGS-34 (Fig. 9a). Blanks contribute to a slight scale contraction in $\delta^{15}N$ of 0.7% at 0.5 mL to 3.4% at 10 mL (see Fig. 8), consistent with observations. By themselves, however, the blanks fail to satisfactorily reproduce observed trends in $\delta^{15}N$ values as a function of aliquot volume (Fig. 9a).

We consider the added influence of incomplete sample sparging on the $\delta^{15}N$ values. From the mean volume-specific N_2O recovery of reference materials among trials relative to that expected (Fig. 2a), we account for isotopic fractionation from the Rayleigh product equation[26] based on the fraction of N_2O remaining in solution after sparging. The observations are reproduced by assigning an N isotope effect for N_2O sparging, $^{15}\alpha_{sparging}$, of 0.9981 (1.9‰; Fig. 9a), admittedly outside our observed range of 0.9987 - 0.9996 (1.3 - 0.4‰). The more substantial isotope effect required to fit the observations may result from the inclusion of anti-foaming agent to sample analyses with bacteria, which was not included in the trials with N_2O aliquots from which the isotope effect estimates were derived (Fig. 4). Alternatively, incomplete bacterial conversion of NO_3^- to N_2O at higher volumes (lower cell concentrations) and associated isotope fractionation could explain the larger $^{15}\alpha_{sparging}$ required to fit the observations. In this regard, we note that the fraction of N_2O recovered in sparging assays (Fig. 4) was noticeably greater than in bacterial assays at corresponding volumes, by 7 ± 7% at 10 mL (Fig. 2a, b). Notwithstanding, this parameterization roughly reproduces the increase in $\delta^{15}N$ of both reference materials from 0.5 to 2 mL, which arises from a tendency for incomplete sparging of the 0.5 mL aliquots as the needle only reached the mere surface of these samples,

while it was submerged with the 2 mL aliquots. It also reproduces the salient decreases in $\delta^{15}N$ at higher sample volumes, similarly borne out of incomplete sparging and potentially incomplete bacterial conversion. This analysis suggests that incomplete N_2O recovery exerts a dominant influence on volume-dependent offsets in ^{15}N, whereas the differential influence of blanks among sample volumes is less important. Bracketing of samples with reference materials of similar volumes provides a mean of accounting for these influences.

We repeat this exercise for $\delta^{18}O$, prescribing an arbitrary $\delta^{18}O$ of 30‰ vs. IAEA-NO3 to the bacterial blank, proportional to the corresponding $\delta^{15}N$ value – assuming equivalent fractionation of industrial NO_3^- due to bacterial consumption.[24] Atmospheric N_2O has a $\delta^{18}O$ of 18.5‰ vs. IAEA-NO3,[25] and we prescribe a value of -23‰ vs. IAEA-NO3 (i.e., 2‰ vs. VSMOW) for the contaminant NO_3^-, also in the natural abundance range. The prescribed O atom exchange with water is 3%. Blanks and O exchange together result in increases in $\delta^{18}O$ of 0.16‰ to 0.45‰ for the 0.5 to 10 mL aliquots of IAEA-NO3, and in more dramatic increases of 2.10‰ to 3.72‰ for the 0.5 to 10 mL aliquots of USGS-34 (Fig. 9b). Accounting for incomplete sample sparging, a prescription of 0.9968 for $^{18}\alpha_{sparging}$ (3.2‰) partly reproduces the trend of the observed $\delta^{18}O$ value changes with volume, but not the magnitude of the changes. Different values of $^{18}\alpha_{sparging}$ do not improve the apparent fit to observations (data not shown), nor do modulations in the $\delta^{18}O$ values of blank sources. Thus, incomplete sparging, blanks and O exchange together fail to adequately reproduce the volume-dependence of $\delta^{18}O$ values. Moreover, invoking incomplete bacterial conversion of NO_3^- to N_2O and associated isotope fractionation do not explain the observed increase in $\delta^{18}O$ scale contraction: With reference to Eq. 10, given a 0.4 nmol N blank, a 10% decrease in the size of a recovered sample relative to an expected 10 nmoles of N results in a negligible increase in scale contraction of ~0.4%. As postulated above, the unexplained offsets in $\delta^{18}O$ and associated scale contraction may arise

from exchange with atmospheric O_2 during denitrification, from fractionation or interferences in the ionization source, or from a process we have yet to surmise.

4. CONCLUSIONS AND RECOMMENDATIONS

We demonstrate that NO_3^- $\delta^{15}N$ and $\delta^{18}O$ values measured with the denitrifier method are subject to volume-dependent offsets. For N isotope ratios, small offsets derive primarily from incomplete sparging of N_2O during sample extraction and associated isotope fractionation during N_2O evasion, and secondarily from bacterial, atmospheric and potentially solution blanks. Incomplete bacterial NO_3^- conversion to N_2O may also be occurring, a notion that merits further investigation. For O isotope ratios, more substantial offsets and scale contraction derive additionally from modest O atom exchange with water and from a yet un-identified (but substantive) process. Contrary to some suppositions, O atom exchange with water was insensitive to sample volume or salinity.

In order to account for volume effects on NO_3^- N and O isotope ratio analyses with the denitrifier method, we advise bracketing NO_3^- samples with reference materials that emulate sample concentrations (volume). Adoption of this practice will ensure higher measurement accuracy and foster inter-comparability among laboratories.

ACKNOWLEDGEMENTS

We thank D. Sigman for insightful discussion of our observations. D. Sigman and A. Weigand also generated some data presented in the manuscript. We are also grateful to Veronica Rollinson and Peter Ruffino for their technical assistance with laboratory and with mass spectrometry analyses. We also thank C. Matassa for the assistance of statistical analyses. This work was supported by CAREER award to JG from the U.S. National Science Foundation (OCE-1554474). Data and meta-data from this study are being archived with BCO-DMO.

REFERENCES

1. Sigman DM, Casciotti KL, Andreani M, Barford C, Galanter M, Böhlke JK. A bacterial method for the nitrogen isotopic analysis of nitrate in seawater and freshwater. *Anal Chem*. 2001;73(17):4145-4153. doi:10.1021/ac010088e
2. Casciotti KL, Sigman DM, Hastings MG, Böhlke JK, Hilkert A. Measurement of the oxygen isotopic composition of nitrate in seawater and freshwater using the denitrifier method. *Anal Chem*. 2002;74(19):4905-4912. doi:10.1021/ac020113w
3. Sigman DM, Granger J, DiFiore PJ, et al. Coupled nitrogen and oxygen isotope measurements of nitrate along the eastern North Pacific margin. *Global Biogeochem Cycles*. 2005;19(4):1-14. doi:10.1029/2005GB002458
4. Beller HR, Madrid V, Hudson GB, McNab WW, Carlsen T. Biogeochemistry and natural attenuation of nitrate in groundwater at an explosives test facility. *Appl Geochemistry*. 2004;19(9):1483-1494. doi:10.1016/j.apgeochem.2003.12.010
5. McMahon PB, Böhlke JK. Regional patterns in the isotopic composition of natural and anthropogenic nitrate in groundwater, High Plains, U.S.A. *Environ Sci Technol*. 2006;40(9):2965-2970. doi:10.1021/es052229q
6. Houlton BZ, Sigman DM, Hedin LO. Isotopic evidence for large gaseous nitrogen losses from tropical rainforests. *Proc Natl Acad Sci U S A*. 2006;103(23):8745-8750. doi:10.1073/pnas.0510185103
7. Knapp AN, Sigman DM, Lipschultz F. N isotopic composition of dissolved organic nitrogen and nitrate at the Bermuda Atlantic Time-series study site. *Global Biogeochem Cycles*. 2005;19(1):1-15. doi:10.1029/2004GB002320
8. Fawcett SE, Lomas MW, Casey JR, Ward BB, Sigman DM. Assimilation of upwelled nitrate by small eukaryotes in the Sargasso Sea. *Nat Geosci*. 2011;4(10):717-722. doi:10.1038/ngeo1265
9. Ren H, Sigman DM, Meckler AN, et al. Foraminiferal Isotope Evidence of Reduced

Nitrogen Fixation in the Ice Age Atlantic Ocean. *Science (80-)*. 2009;323(5911):244-248. doi:10.1126/science.1165787

10. McIlvin MR, Casciotti KL. Technical Updates to the Bacterial Method for Nitrate Isotopic Analyses. *Anal Chem*. 2011;83(5):1850-1856. doi:10.1021/ac1028984
11. Weigand MA, Foriel J, Barnett B, Oleynik S, Sigman DM. Updates to instrumentation and protocols for isotopic analysis of nitrate by the denitrifier method. *Rapid Commun Mass Spectrom*. 2016;30(12):1365-1383. doi:10.1002/rcm.7570
12. Coplen TB, Böhlke JK, Casciotti KL. Using dual-bacterial denitrification to improve δ15N determinations of nitrates containing mass-independent 17O. *Rapid Commun Mass Spectrom*. 2004;18(3):245-250. doi:10.1002/rcm.1318
13. Tanaka N, Rye DM, Rye R, Avak H, Yoshinari T. High precision mass spectrometric analysis of isotopic abundance ratios in nitrous oxide by direct injection of N2O. *Int J Mass Spectrom Ion Process*. 1995;142(3):163-175. doi:10.1016/0168-1176(94)04100-L
14. Braman RS, Hendrix SA. Nanogram Nitrite and Nitrate Determination in Environmental and Biological Materials by Vanadium(III) Reduction with Chemiluminescence Detection. *Anal Chem*. 1989;61(24):2715-2718. doi:10.1021/ac00199a007
15. Shrivastava A, Gupta V. Methods for the determination of limit of detection and limit of quantitation of the analytical methods. *Chronicles Young Sci*. 2011;2(1):21. doi:10.4103/2229-5186.79345
16. Inoue HY, Mook WG. Equilibrium and kinetic nitrogen and oxygen isotope fractionations between dissolved and gaseous N2O. *Chem Geol*. 1994;113(1-2):135-148. doi:10.1016/0009-2541(94)90009-4
17. Bourg IC, Sposito G. Isotopic fractionation of noble gases by diffusion in liquid water: Molecular dynamics simulations and hydrologic applications. *Geochim Cosmochim Acta*. 2008;72(9):2237-2247. doi:10.1016/j.gca.2008.02.012
18. Casciotti KL, Böhlke JK, McIlvin MR, Mroczkowski SJ, Hannon JE. Oxygen isotopes in

nitrite: Analysis, calibration, and equilibration. *Anal Chem*. 2007;79(6):2427-2436. doi:10.1021/ac061598h

19. Buchwald C, Casciotti KL. Isotopic ratios of nitrite as tracers of the sources and age of oceanic nitrite. *Nat Geosci*. 2013;6(4):308-313. doi:10.1038/ngeo1745
20. Casciotti KL, McIlvin M, Buchwald C. Oxygen isotopic exchange and fractionation during bacterial ammonia oxidation. *Limnol Oceanogr*. 2010;55(2):753-762. doi:10.4319/lo.2010.55.2.0753
21. Boshers DS, Granger J, Tobias CR, Böhlke JK, Smith RL. Constraining the Oxygen Isotopic Composition of Nitrate Produced by Nitrification. *Environ Sci Technol*. 2019;53(3):1206-1216. doi:10.1021/acs.est.8b03386
22. Weiss RF, Price BA. Nitrous oxide solubility in water and seawater. *Mar Chem*. 1980;8(4):347-359. doi:10.1016/0304-4203(80)90024-9
23. Granger J, Sigman DM, Prokopenko MG, Lehmann MF, Tortell PD. A method for nitrite removal in nitrate N and O isotope analyses. *Limnol Oceanogr Methods*. 2006;4(7):205-212. doi:10.4319/lom.2006.4.205
24. Granger J, Sigman DM, Lehmann MF, Tortell PD. Nitrogen and oxygen isotope fractionation during dissimilatory nitrate reduction by denitrifying bacteria. *Limnol Oceanogr*. 2008;53(6):2533-2545. doi:10.4319/lo.2008.53.6.2533
25. Prokopiou M, Sapart CJ, Rosen J, et al. Changes in the Isotopic Signature of Atmospheric Nitrous Oxide and Its Global Average Source During the Last Three Millennia. *J Geophys Res Atmos*. 2018;123(18):10,757-10,773. doi:10.1029/2018JD029008
26. Mariotti A, Germon JC, Hubert P, et al. Experimental determination of nitrogen kinetic isotope fractionation: Some principles; illustration for the denitrification and nitrification processes. *Plant Soil*. 1981;62(3):413-430. doi:10.1007/BF02374138

Table 1. Linear regressions of N_2O peak areas, $\delta^{15}N$ and $\delta^{18}O$ values vs. aliquot volume of DIW (Trials 1-5) and seawater (Trial 6, Weigand trials). The respective slopes (± the standard error), coefficients of determination (r^2) and the statistical significance of the slopes are shown. Statistically significant relationships are denoted with asterisks (p-value ≤ 0.05*; ≤ 0.01**)

	Trial	Slope	r^2	p-value
N_2O Peak Area (Vs)	1	-0.22 ± 0.03	0.82	**
	2	-0.06 ± 0.03	0.13	0.07
	3	-0.19 ± 0.04	0.41	**
	4	-0.16 ± 0.09	0.13	0.08
	5	-0.05 ± 0.02	0.32	**
	6	-0.06 ± 0.02	0.37	**
	Weigand 2 nmol N	-0.02 ± 0.02	0.12	0.19
	Weigand 3 nmol N	-0.08 ± 0.02	0.49	**
$\delta^{15}N$ (‰ vs. N_2O_{ref})	1	-0.02 ± 0.01	0.27	*
	2	-0.03 ± 0.00	0.73	**
	3	-0.01 ± 0.00	0.16	*
	4	-0.01 ± 0.00	0.13	0.08
	5	-0.01 ± 0.00	0.31	**
	6	0.00 ± 0.01	0.02	0.56
	Weigand 2 nmol N	-0.02 ± 0.01	0.12	0.18
	Weigand 3 nmol N	-0.02 ± 0.01	0.21	*
$\delta^{18}O$ (‰ vs. N_2O_{ref})	1	-0.15 ± 0.02	0.87	**
	2	-0.17 ± 0.01	0.94	**
	3	-0.10 ± 0.02	0.46	**
	4	-0.01 ± 0.01	0.03	0.45
	5	-0.01 ± 0.05	0.00	0.76
	6	-0.04 ± 0.02	0.11	0.12

	Weigand 2 nmol N	-0.02 ± 0.03	0.05	0.42
	Weigand 3 nmol N	-0.02 ± 0.02	0.05	0.33

Table 2. Linear regressions of N_2O blank amplitudes vs. aliquot volume in DIW and seawater trials with *P. aureofaciens* and *P. chlororaphis*.

Strain	Trial	Aliquot	Intercept	Slope
P. aureofaciens	190321	SW	0.08	0.032
	190905	SW	0.05	0.023
	190510	SW	0.06	0.024
	200607	DIW	0.04	0.015
	200607	SW	0.02	0.016
	Weigand	SW	0.08	0.025
P. chlororaphis	190314	SW	0.05	0.019
	190307	SW	0.16	0.008
	190419	SW	0.05	0.040
	200608	DIW	0.03	0.014
	200608	SW	0.02	0.011

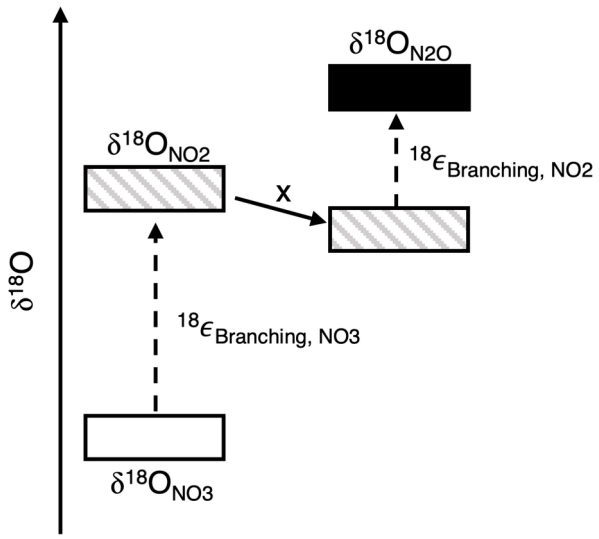

RCM_9224_Figure 1.tif

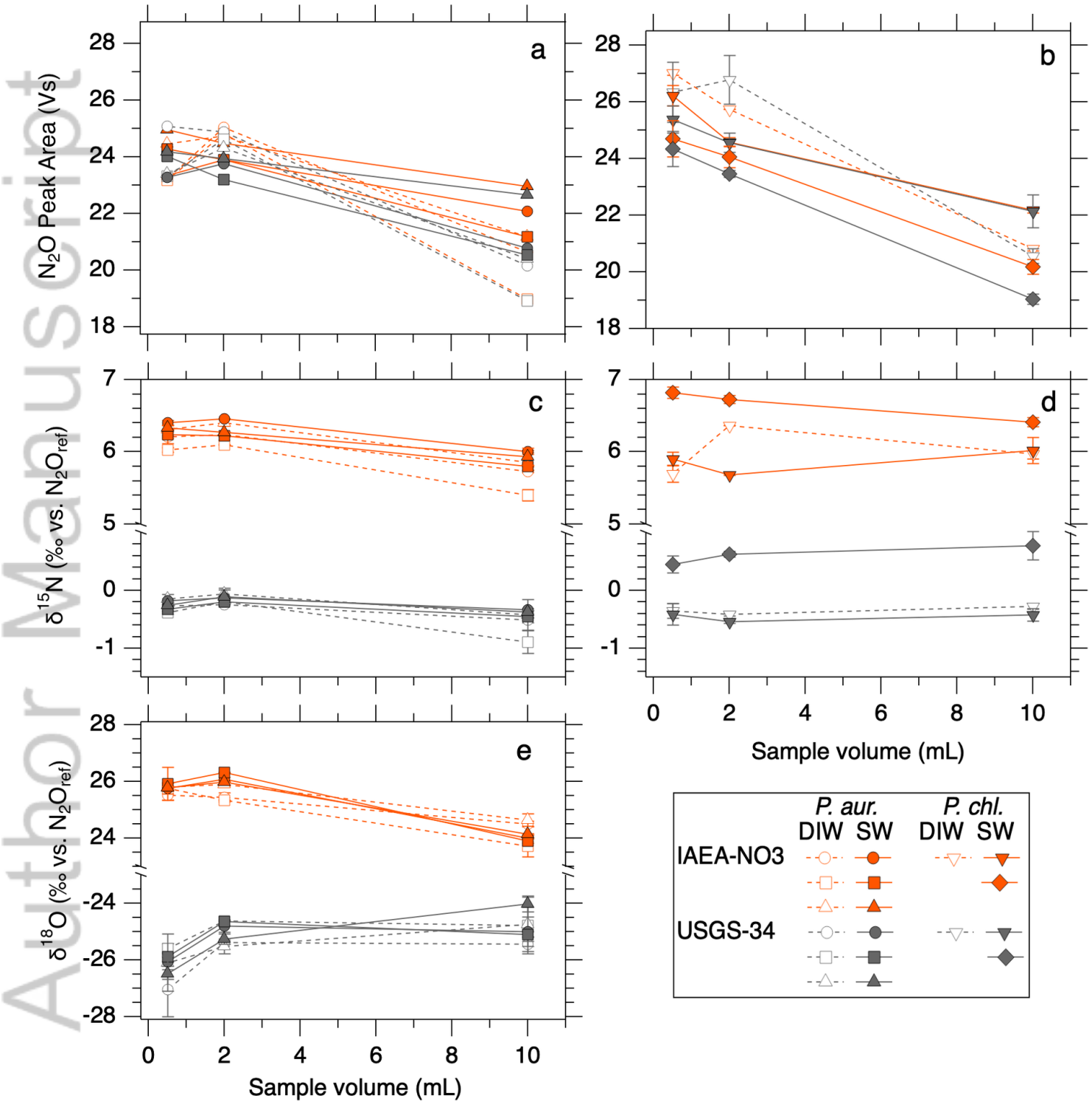

RCM_9224_Figure 2.tif

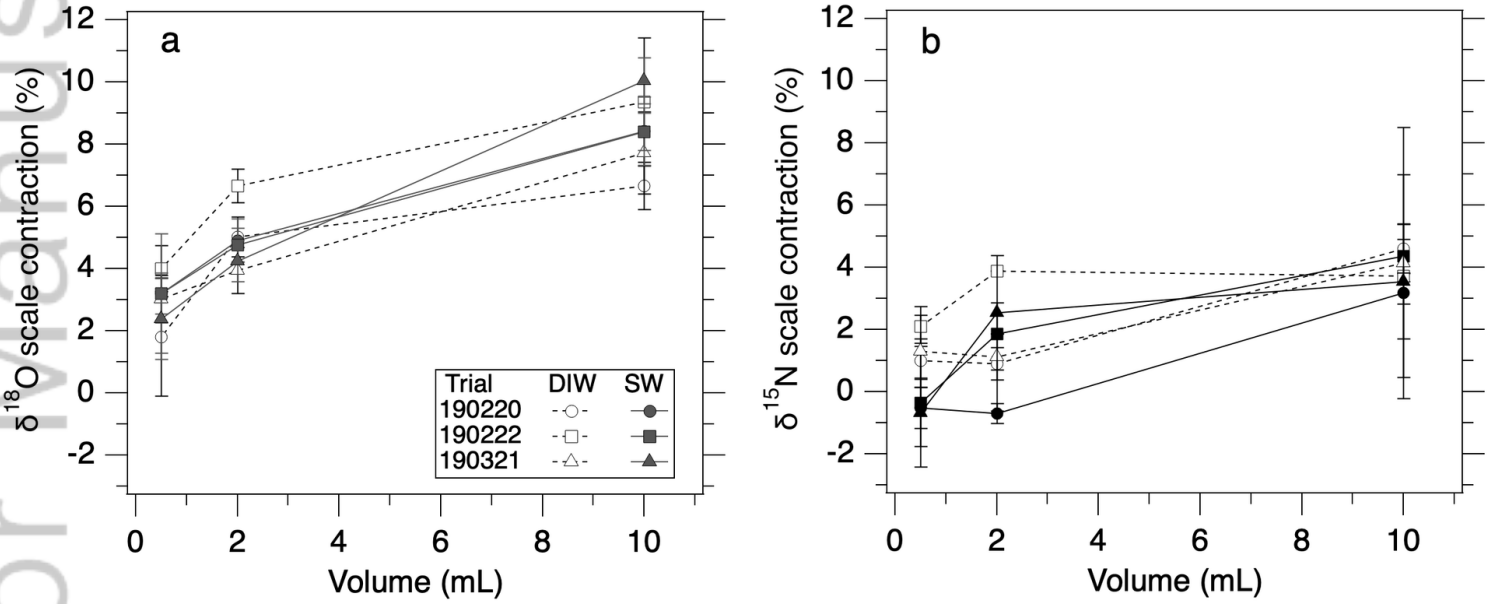

RCM_9224_Figure 3.tif

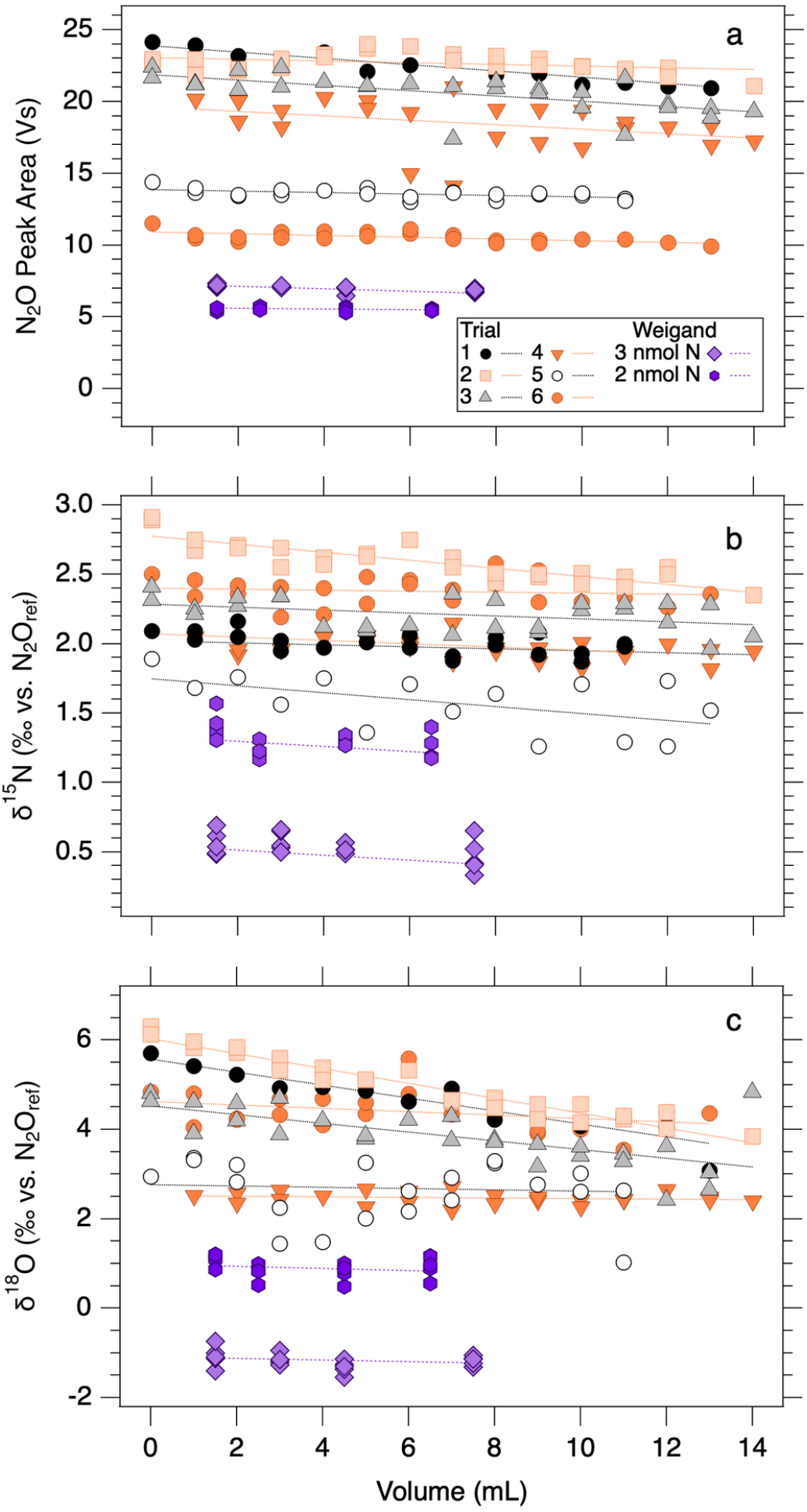

RCM_9224_Figure 4.tif

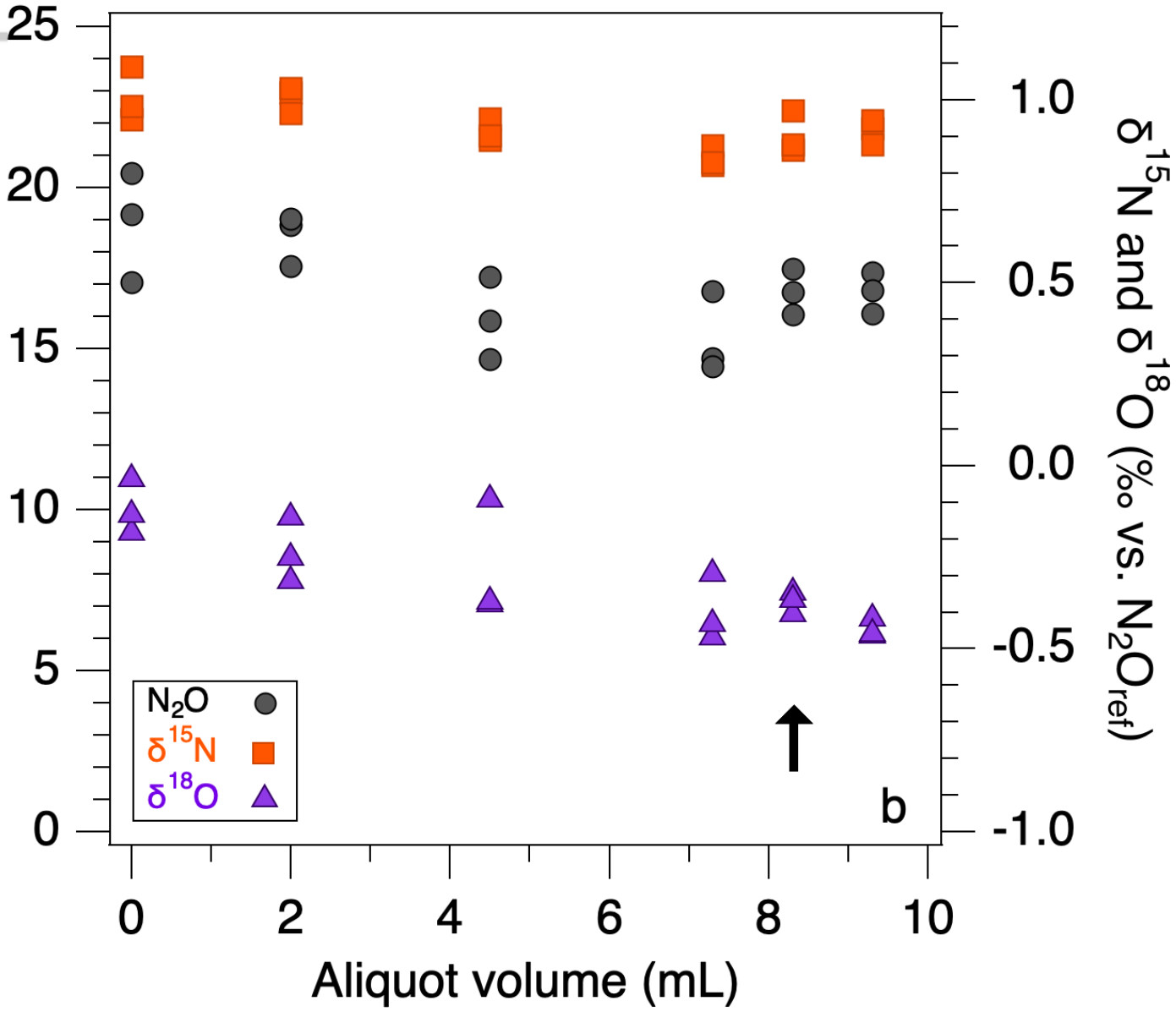

RCM_9224_Figure 5.tif

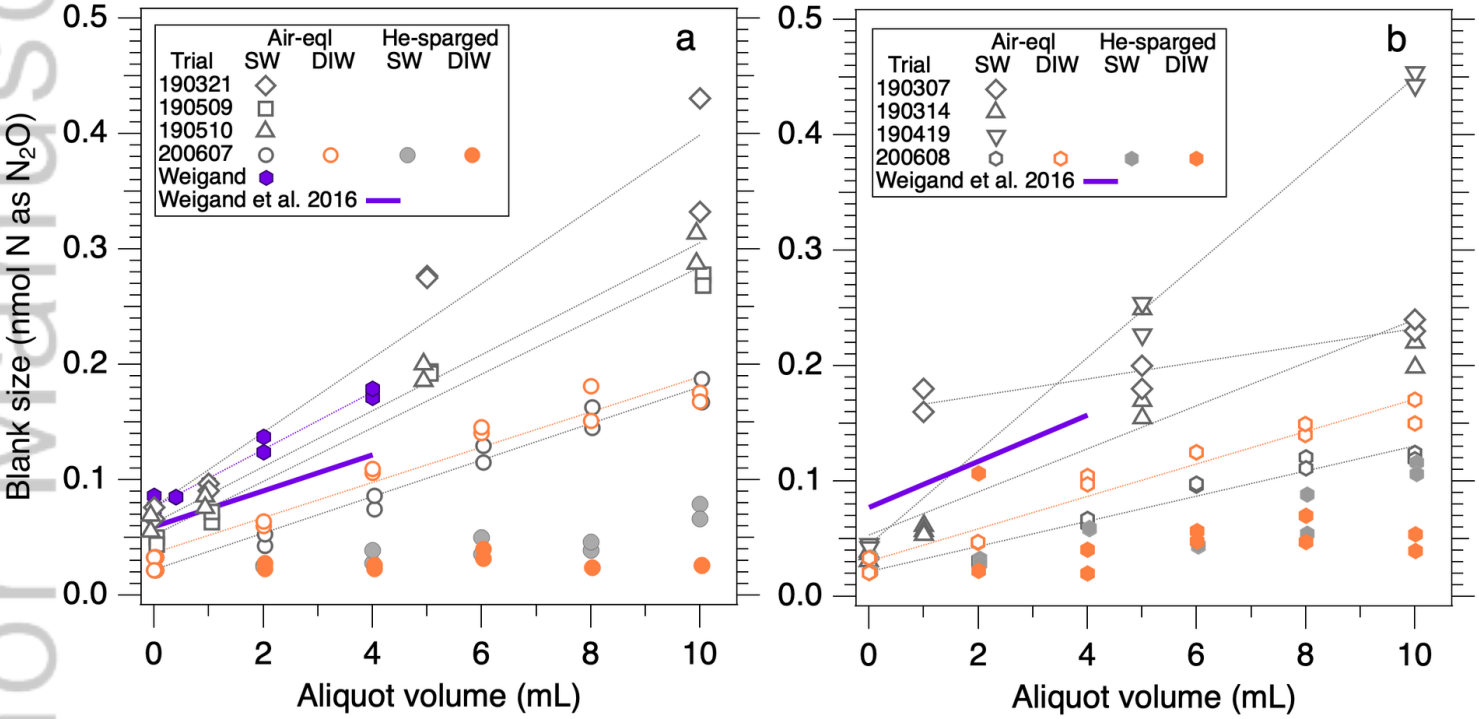

RCM_9224_Figure 6.tif

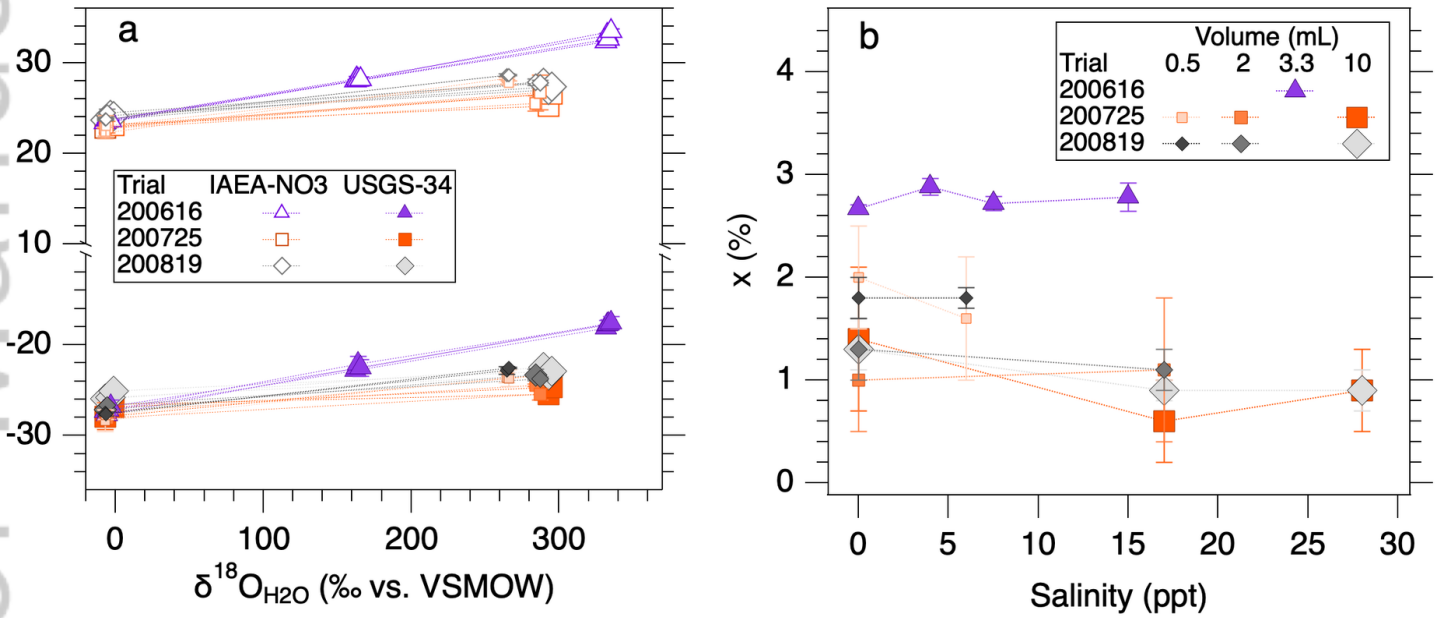

RCM_9224_Figure 7.tif

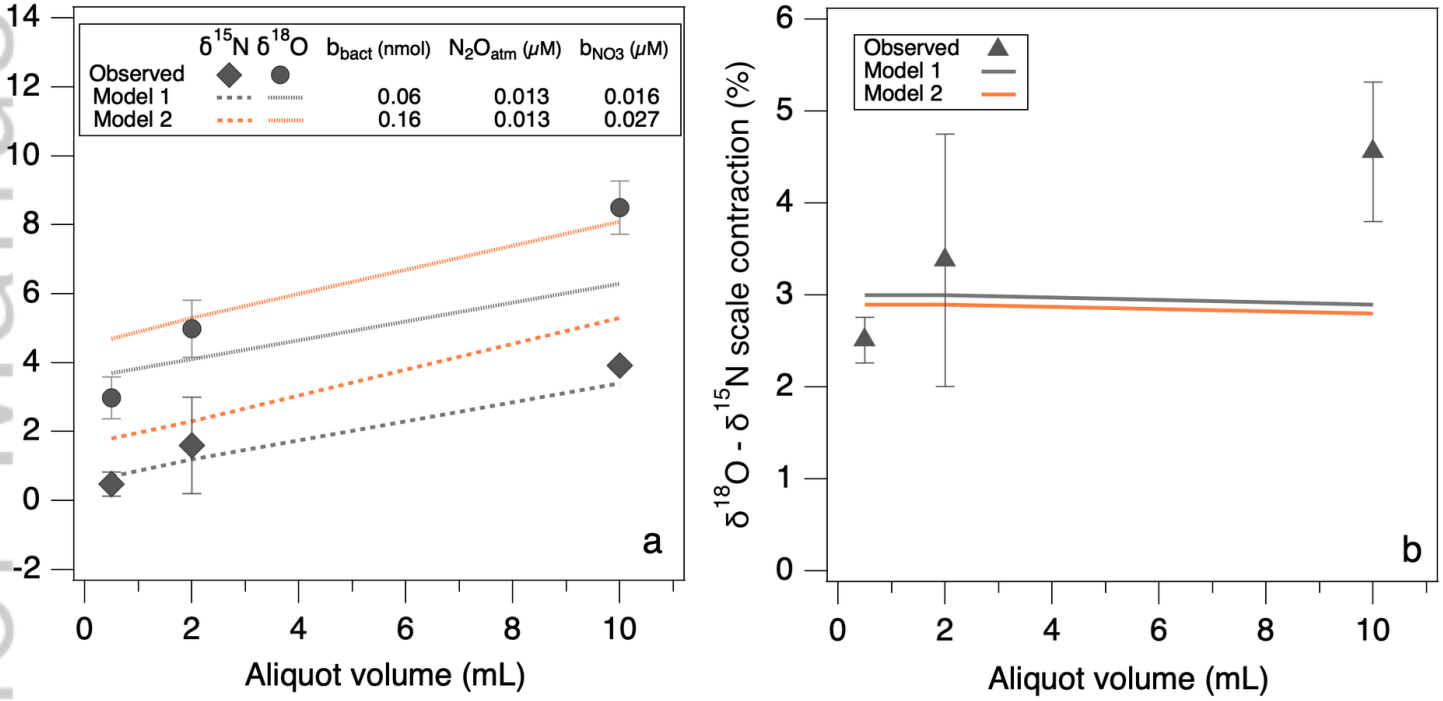

RCM_9224_Figure 8.tif

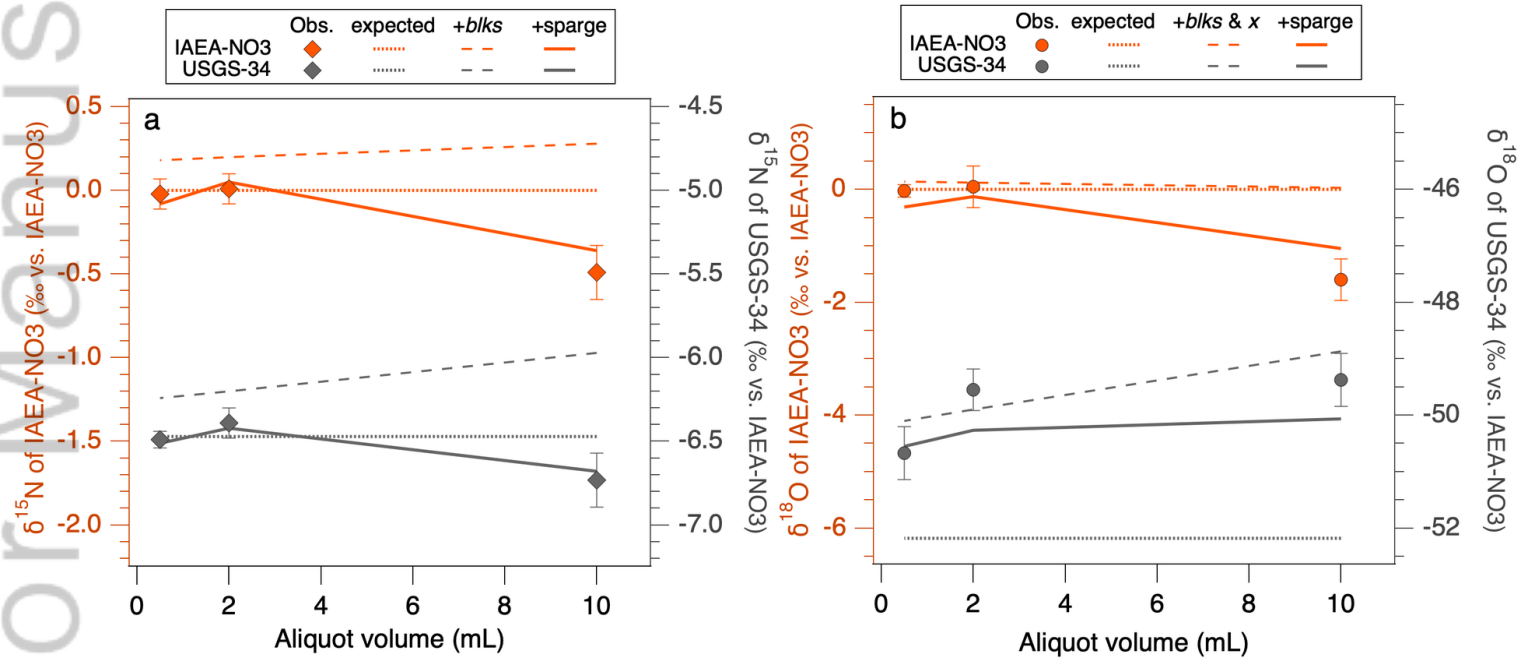

RCM_9224_Figure 9.tif